Annals of R.S.C.B., ISSN:1583-6258, Vol. 25, Issue 4, 2021, Pages. 4919 - 4942
Received 05 March 2021; Accepted 01 April 2021.

Ultra-Low Energy-Efficient Programmable Array Accelerator and Compiling Flows for the Near Sensor

Siva Sankara Phani. T[1], M. Durga Prakash[2]

[1] Department of ECE, Koneru Lakshmaiah Education Foundation, Green Fields, Vaddeswaram, Guntur 522502,AP,India
[2] Department of ECE, V R Siddhartha Engineering College(Autonomous), Kanuru, Vijayawada 520007,AP,India

Abstract

We present the ultra-low-energy accelerators for near-sensor handling Coarse grained reconfigurable arrays (CGRAs). The Integrated Programmable Array Accelerator (IPA) in application kernels containing complex controller flows, with an overhead of powerful cutting-edge approaches, provides a new architecture, model execution, and compilation flow. In order to improve performance and productivity, our research builds on IPA architecture with common memory access in this paper. Compared to the most advanced partial and full prediction methods, we are making maximum energy and efficiency gains. Compared to the center of ultra-low capacity near-sensor processing via a large number of near sensor kernels, the proposed accelerator would achieve high energy efficiency.

Keywords:CGRA, compilation, CDFG, ultralowpower accelerator

1.Introduction

Due to the increasing complexity of near sensor data algorithms, high power and extreme energy demands for low power, embedded applications such as wireless sensor networks, Internet of Things (IoT), and wearable sensors are combined in mW power packages. The conventional low-power processing system is based on hardwired architectures from the Application Specific Integrated Circuit (ASIC). The core power during processing is versatile, but traditional overhead processing instructional processing [1] is connected to overhead power, coding and data path (up to 40%), overhead loading and storage (up to 30 percent). In this work we make major steps to energy efficiency by applying the CGRA architectural template and overhauls that fit the ultra-moderate power envelope in application-specific knowledge pathway (mW). CGRAs have, in the past, been extensively studied in mobile (hundreds of mW)[2] for high-performance applications using electricity consumption profiles. In this post, we focus on CGRAmW

Annals of R.S.C.B., ISSN:1583-6258, Vol. 25, Issue 4, 2021, Pages. 4919 - 4942
Received 05 March 2021; Accepted 01 April 2021.

architecture (and below). In this ultra-low-power mission profile, few CGRA architectures were pressed [3]. The goal is to speed up the use of L1 to share a PULP processor group[4]. A powerful CGRA is the accelerator. Thus, the efficient sharing of L1 memories is another major problem in this context. It is necessary that ample memory be shared to minimize disputes over memory access. The number of port connected to the logarithmic interconnection to L1 memory must be strictly limited, on the other hand, to prevent large areas and power overheads. We are using the Integrated Programmable Arrangement Accelerator (IPA), which was proposed at [5] in connection with a multi-bench scaled and configurable database memory hierarchy to overcome very low power and memory sharing challenges. The TCDM is also a multi-bank press. Architecture is a key benefit for comparing shared memory data with a typical parallel processor class with the use of kernel as opposed to data-efficient data. This is a major advantage in kernel running data communication between processing elements (PEs). On the shown sample programme the IPA cluster performs less memory operations. ie, the energy level is 1.3 times greater than the multimedia cluster that transmits the data via TCDM. In order to provide ease, we also disregard barrier overhead synchronization in the multi-core cluster. The IPA approach considerably reduces memory pressures and thus complicates the relations between PEs and memory banks since a smaller number of banks are sufficient for the low-fighting needs. On CGRAs, the data exchange between nuclei takes place using parallel OpenMP data structures and shared structures, rather than the clustered multi-core architectures to minimize access to common memory, and the compiler is responsible for ensuring data exchange between PEs, using point-by-point links between PEs as much as possible. The building of CGRA's energy efficiency needs control of loop-based information and control dependency is also a major challenge. For CGRAs, only certain percentage concerns the straight line (basic block) coding sequence of the innermost loop. For conditional in the innermost loop, compilers are converted into control flows in data flow structures using predictive techniques [6]. These compilers can only generate code for running a single loop, as many pipelines are running a number over and over again (loop boundaries = number of piped stages). Only the innermost loop is accelerated when the loops are nestled by a CGRA, leaving external loops for the host processor. However, more CGRA synchronization and communication memory mapping operations are required for several hostsdownload. This leads to significant overheads, particularly when the innermost circuit contains very few iterations; a typical scenario for sensor applications. Wide high-level

Annals of R.S.C.B., ISSN:1583-6258, Vol. 25, Issue 4, 2021, Pages. 4919 - 4942
Received 05 March 2021; Accepted 01 April 2021.

CGRA architectures also employ predictive techniques to reveal the reliance on concurrent monitoring. The forecasts unfortunately lead to a loss of resources, and in a strong and region controlled situation [7] it is difficult to justify them. We solve these problems in this paper with the new building flow adapted to our low-power IPA architecture. This flow utilised for enforcing a certain number of loops or conditionality in the ANSI C code, using the energy efficient allowance form. This paper outlines the two major aspects of CGRA mapping energy conservation. To optimize performance and energy usage, we first of all perform an architectural survey based on the IPA. The IPA completely supports conditional transactions, operates the PE internal intermediate data exchange registers, and uses a TCDM multi-bank buffer access, thereby improving substantial electricity efficiency. Secondly, it defines a complete multi-loop compile flow and IPA map kernels. The flow helps the host processor to measure external loops and increases the IPA performance significantly. It also offers high energy efficiency by reducing architectural elements for the amount of memory operations. We compare output with existing prediction approaches to IPA in order to calculate the efficiency of the IPA architecture and compilation flux. In the register assignment process, control intensive core tests showed maximum output of 1.33x (at least 1.04x with an average of 1.13x) and 1.8x (at least 1.37x and 1.59x average) compared to partial predicting and completely predicting. This is shown as the main performance gain. We examined the efficiencies and power optimization of the bank factor 0,5 with an IPA configuration with 4x4 PEs in optimizing conventional L1 memory access (e.g. 8 LSUs, 4 TCDM banks). In addition, the IPA has a very common layout and functional data path, ideal for control of fine grain strength. Our standard architecture enables us to create a mechanism for the grain clock gating that increases the non-clock-driven IPA to 2 on average. The results show that the IPA is 20.3x high and averages 9.7x over an area of 1 to 1000. The IPA has an average power of up to 1617 MOPS/mW of 0.6V and on average is up to 18 times that of the processor.

2.Literature Survey

A lot of research has been conducted into the performance, efficiency and cost of CGRAs [8]. This paper focuses on the architectural and energy conservation aspects. Because of low power efficiency, data and context management are extremely necessary. CGRAs have been incorporated in a number of solutions in recent years into data and memory education

Annals of R.S.C.B., ISSN:1583-6258, Vol. 25, Issue 4, 2021, Pages. 4919 - 4942
Received 05 March 2021; Accepted 01 April 2021.

accelerators. The host processors perform memory tasks in several CGRAs [9]. This includes the Samsung High Speed Processor (CMA) of up to 3 mW. Only when arranged via the processor in shared registry format are PEs able to access data in this architecture. The main issue of energy efficiency is the efficiency of the supply of CPU data and the measurement of PE. The numerical effect of the PE array is, however, also affected by the processor due to high overheads of synchronization. For example, in ADRES, the VLIW processor controls access to data mematics up to 20% of the overall power. The host CPU uses CMA to add a common registry file to the PE data (FR). This is rather negative with respect to versatility. In order to balance processor parameters and processor power, the efficiency and bandwidth requirement is modified, this architecture's main goal is to create an autonomous DVFS (52) or corpsenaldistance. The highest energy efficiency in a CMA is 743 MOPS/mW for 8-bit kernels. There is no mention of the overhead controller. We intend to use the C-to-CGRA to compile end-to-end data and application kernels in the language of C as the only job for the customized DFG specified in that job. For MorphoSys; RSPA; SmertCell; PipeRench; Simid-CGRA, POSs shall be directly liable for load-storage operations. In the standard storage, data elements are stored in these architectures using the PE line memory port. The major disadvantage of data Access Architecture is the high-priced shares of the data among rows over complex array networks between the same set of PE in memory bank access. We use a multi-bank common mematics that connects to a word point in order to minimize conflicts with these architectures. The data sharing between tiles is based on a very simple point-to-point communication infrastructure or a versatile generic TCDM. NASA and FPPA RDPP are designed to handle spacecraft with low energy. Centered on these architectures are the data stream and the synchronous model of data stream that prevents memory and control investments. But the IPA was adapted with a workload that differs greatly from the processing of stream data for effective energy processing. Table 1 provides the overview of the CGRA feature and architectural approaches. CPU uploading, sync, and intruder computing are all part of the kernel speed. The table shows that both internal and external loops are carried out via IPas, with less total contacts and memory operation performed by the kernel memory. It shows that the PE has random access to local memory in a highly energetic generic IPA speed control device, as well as complete controlling and data flow on this state of the art re-set array and processor portfolio, based on the generic ANSI-C application. In order to assess if the LSU and the memory share bank numbers are optimal, this paper also

Annals of R.S.C.B., ISSN:1583-6258, Vol. 25, Issue 4, 2021, Pages. 4919 - 4942
Received 05 March 2021; Accepted 01 April 2021.

focuses on improving the proposed IPA accelerator. We will deal with this topic in this article. In addition, an average 2 x improvements in energy efficiency allows the dynamic consumption of idle tile during kernel performance to be avoided by fine-grain power management. The worldwide low-cost and scaled data memory system and an extensive architecture for seed power control explain what the accelerator is for the proposed Ultra-Low-Power PC architecture.

CGRA compiler loops have been mainly mapped with software [10]. The pipeline can be used for the inner part of the loop. In comparison, the CPU can cause any outside loop iteration in the CGRA that provides a substantial overhead for CGRA-CPU synchronization. As demonstrated by Liu et al [11], polyhedral loops were split into two levels. This form, however, is not universal since arbitrary loops are hard to estimate. A kernel loop is used in some approaches [12]. The underlying theory is that the innermost loops are not enough to fly. The solutions are increasingly interrupting the intimate circuits. The host must perform the external loops. As most of the compilers suggested that a kernel's internal loop was to be used, partial predictions and general predictions are key techniques for mapping conditional elements in the loop. Some forecast charts for different PEs, whether or not. If all sections and other variable adjustments are based on a branch status evaluation, the outcome is calculated by selecting the output from the relevant instructions. This technology strengthens the use of PE as both paths are conditionally used to maximize energy consumption. In absolute forecast, unlike partial forecasts, all instructions are predicted. Directions are taken on each PE flow path if the predicate value of the instructions is the same as the PE flag. There are no incorrect path directions executed. The number of roads degrades the technology's lateness and energy efficiency. Full forecasts are revised [13] under state-based conditions. Sleep and waking problems are not ignored, but efficiency is not improved. Both PE Instructions have a dual problem [14] of energy efficiency, one from one direction and another. The second point concerns the conservation of oil. This method is compared to partial predictions of energy efficiency. However, this approach is too restrictive in view of unbalanced and nesting conditions. An unbalanced state map and a single loop on CGRA display the trigged architecture of the long instruction system [15] (TLIA). The procedure fuses into triggers all kernel requirements and produces a collection of instructions for each command. With the depth of nesting conditions, the efficiency of this system decreases. The TLIA solution has reached the bottleneck in relation to the loop nesting, which fulfillsseveral instructions in the small PE range. Registry assignment [16] is the proposed type

Annals of R.S.C.B., ISSN:1583-6258, Vol. 25, Issue 4, 2021, Pages. 4919 - 4942
Received 05 March 2021; Accepted 01 April 2021.

of compilation for mapping the CDFG to the CGRA. Both loops and conditions can be mapped at any depth in this way. The limit of kernel mapping is in this case limited to the PE command and not to the programme structure (i.e. number of loops, and branches). The size of a managed CGRA code segment can increase to a limit which in other methods is not trivial, reduces control and overhead cardiac synchronization. Table 2 provides a detailed comparison among the kernel flow control techniques. The main purpose is to draw the innermost loop using software and loop release pipelines and one of them is to track the branch inside the loop. Consequently, hybrid mapping solutions are used for new compilers. To find the right balance, it would be easier to evaluate the target architecture and application domain. Conversely, in our proposed construction flow, all conditions and loops can be efficiently processed.

Table 1: Overview of the CGRA feature and architectural approaches

References	[9]	[11]	[17]	This paper
Memory	CPU	CGRA	CPU	CGRA
Innermost loops	CGRA	CGRA	CGRA	CGRA
Outer loops	CPU	CPU	CGRA	CGRA
Offload+sync	CPU	CPU	CPU	CPU

Table 2: Detailed comparisons among the kernel flow control techniques

Techniques	Conditionals		Loops	
	Balanced	**Imbalanced**	**Single**	**Nested**
Partial Predication	Yes	Yes	No	No
Full predication	Yes	Yes	No	No
State based full predication	Yes	Yes	No	No
Dual issue single execution	Yes	No	No	No
TLIA	Yes	Yes	Yes	No
Software Pipelining	No	No	Yes	No

Annals of R.S.C.B., ISSN:1583-6258, Vol. 25, Issue 4, 2021, Pages. 4919 - 4942
Received 05 March 2021; Accepted 01 April 2021.

Loop Unrolling	No	No	Yes	NA
Register allocation	Yes	Yes	Yes	Yes

3.Overview of Execution Model

When the kernel has been compiled, the compiler produces the installation and addresses for the locally shared memory inputs and outputs. The assembler uses assembly and ISA for created a background for each PE, which is preloaded to the GCM, i.e. software which is stored in the IRF. The past of each PE in the array comprises instructions and constants. The background is loaded in the corresponding IRF and CRF PEs before execution starts. Your local warehouse is supposed to match the code. For broader context management, the IPA controller and the overlays may be used. In order to be succinct, specifications of this method are omitted. Each loop includes 20-bit local IRF instructions. The immediate data is transferred to a permanent registry file that simplifies compression. Consequently, the decoder pressure is very low. Figure 1 demonstrates typical CPU and IPA sample programme output. The sample programme instructions for CPU and IPA are 31 and 12. In addition, during the sample running the IPA provides 28x Processor performance gains. This is mostly because of a considerably lower number of memory operations, and because the small loop will roll completely without the size of the blown-up code.

Annals of R.S.C.B., ISSN:1583-6258, Vol. 25, Issue 4, 2021, Pages. 4919 - 4942
Received 05 March 2021; Accepted 01 April 2021.

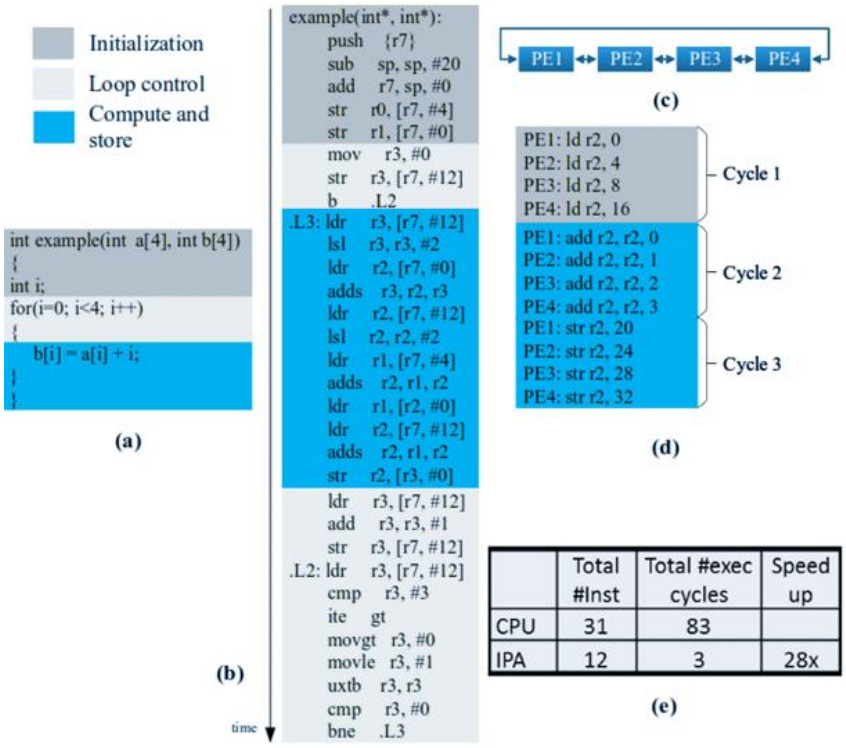

	Total #Inst	Total #exec cycles	Speed up
CPU	31	83	
IPA	12	3	28x

Figure1: Sample code

The sample programme and the respective CDFG are shown in Figure 2. The basic blocks are shown as blue rectangles in this diagram. A black fleet is the flux from a main block to a second fundamental block. Strong and breached arrows demonstrate the real and false ways of a controlled cjmp. This illustrates how the implementation of the CDFG flows.

BB_1→ BB_2→(either BB_3 or BB_8) if BB_3→BB_4→(either BB_5 or BB_6)→BB_7……

The PEs in the array must be aligned with the same basic block to retain the execution flux. Since all PEs in the PEA have to use a basic element since the running stream hops from one element to another. You can run all PEs in a single block, simultaneously or sequentially. The same PE can be used every day for a variety of simple blocks. The programmer can programme different operations and data on the same PE with synchronized execution. We subsequently present the CDFG model with the application model, to help with the compilation flow in various stages.

Annals of R.S.C.B., ISSN:1583-6258, Vol. 25, Issue 4, 2021, Pages. 4919 - 4942
Received 05 March 2021; Accepted 01 April 2021.

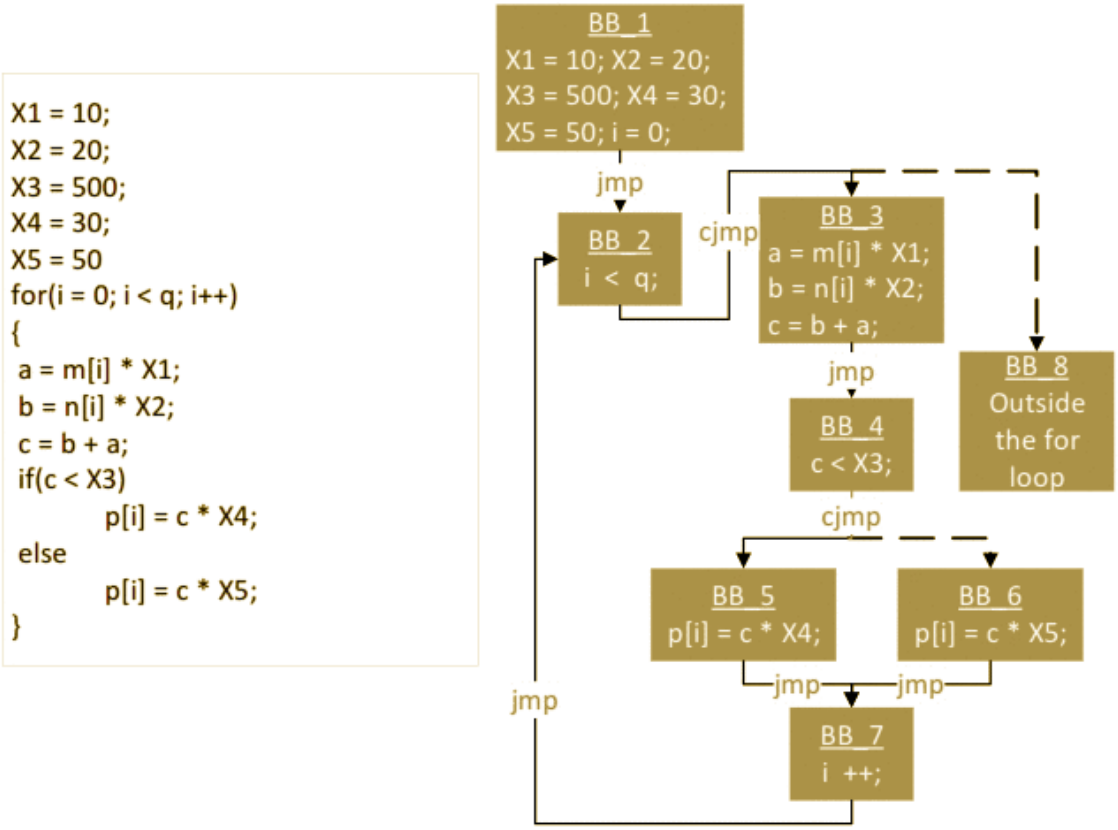

Figure 2: CDFG Sample Code

Annals of R.S.C.B., ISSN:1583-6258, Vol. 25, Issue 4, 2021, Pages. 4919 - 4942
Received 05 March 2021; Accepted 01 April 2021.

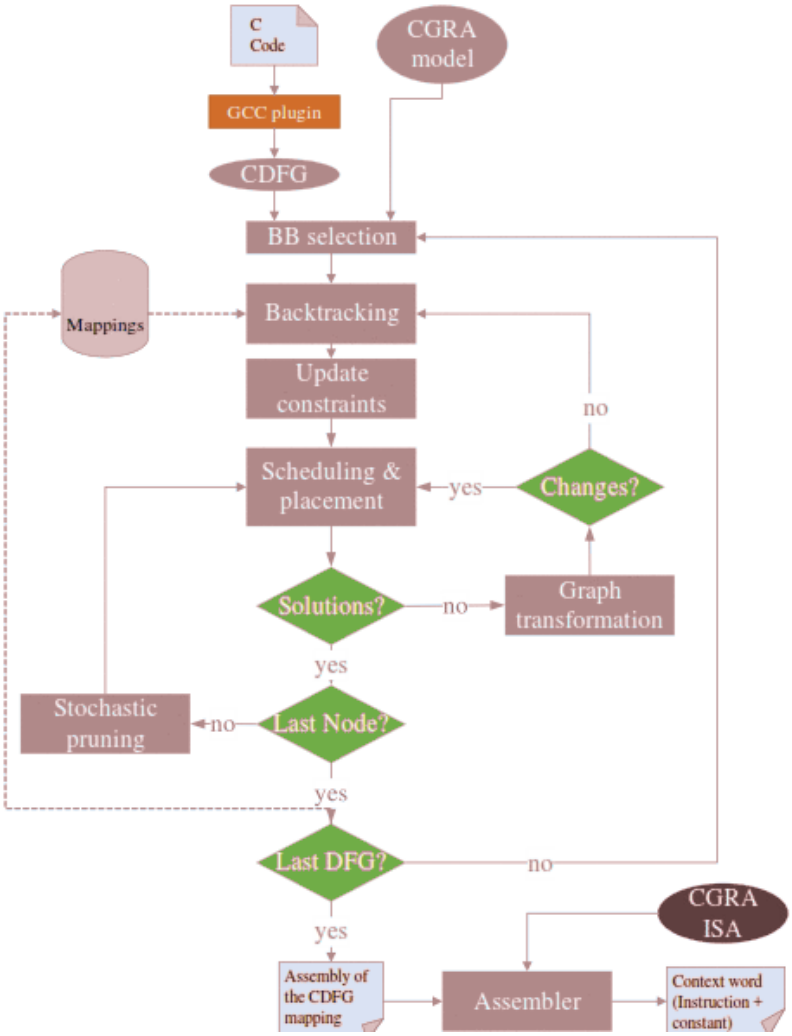

Figure 3: Compilation diagram

The schematic representation of CDFG mapping to PEA can be shown in Figure 3. The maps of CDFG are compatible with a set of DFG mappings. DFGs must view the PE data at the same location in order to be reliable. The allocation process of the register ensures that. For the basic blocks described in [18] our mapping method is very scalable and effective. This document improves the compilation process of DFG mappings, which can be modified by registry assignment to map the entire CDFG to a PE array. As shown in Figure 3, the entire compilation stream consists of six stages: BB collection, monitoring, updating limitations, schedules, placement, conversion of the graph, and stochastic pruning.

In the following sub-sections, these operations are detailed.

Annals of R.S.C.B., ISSN:1583-6258, Vol. 25, Issue 4, 2021, Pages. 4919 - 4942
Received 05 March 2021; Accepted 01 April 2021.

1) Scheduling:

A list of algorithms to plan the DFG is used for each single block. It is based on a heuristic in which priority orders are specified for schedulable operations. A node is planned when reversed and all its children are scheduled. Traditional memory nodes and nodes can be processed differently. Furthermore, if different nodes have equal mobility, the second priority criterion shall be the number of their descendants. More heirs are the higher the priority. In fact, because of the routing constraints of the restricted links between tiles, a node with a larger number of successors is more difficult to map. The planning of these nodes therefore usually allows the latency to be reduced [19]. In the PE model list, the compiler tries to find a place before the highest priority node is found. If the positioning solution exists, the graph would otherwise be converted into the node. The placement is based on a new Levi algorithm edition. The algorithm proposed adds to the subsection already designed and placed nodes the newly designed operating node and its relevant data node. The two nodes could only be added without paying attention to the previous solutions and the TLC. When there is no solution, all of the previous partial solutions to this pair are hard to connect since the Levi algorithm offers a complete solution for exploration of space. Graphs must be transformed in this situation.

2) Transformation of graph:

When no binding solution is found, DFG is transformed dynamically. For our compilation flow, the three graph transformations are used. The procedure is divided into a working node with the same input and output ranges distributed to minimize the number of successors to the original operating node. Memorization routing adds a saving node and a corresponding data node for halting a transaction and ensuring data reliability. The routing task adds a task node to increase the physical gap between the source variables and the dropdown symbol by one. As a consequence of TLC or RLC, the DFG dynamically increases the physical distance between a vector-source symbol and a sink to one.

3) Pruning:

Too many partial charts contribute to the precision of the positioning method. If it is not cut, it grows exponentially. Thus, we use the stochastic pruningmethod.

Annals of R.S.C.B., ISSN:1583-6258, Vol. 25, Issue 4, 2021, Pages. 4919 - 4942
Received 05 March 2021; Accepted 01 April 2021.

4) Selection of a block:

The compiler selects one mapping from the different mappings after planning and linking all nodes of the base block. As already suggested, multiple block mappings must protect the integrity of data.Since it is important to select fundamental blocks during mapping, several CDFGs are compared in this section by the number of RLCs and TLCs. Table 3 compares the number of CDFRGs for the first major search (BFS) and for the first major search (DFS). Table 3 indicates the reverse constraints. This is listed in the table below. Since the model is identical to other kernels, only 2D filters are available in sob and partition. Statistics show that, forwards and reverse, DFS produces less RLC than BFS. Due to the many sequence loops present in the kernel, the RLC number for sobel filters in BFS is considerably higher. The TLC numbers for various crossing mechanisms are identical in both approaches. In various search methods related results are also used. This is used in the DFS technique.

Table 3: Comparison of RLC and TLC with various CDFG

Kernels	Forward Traversal				Backward Traversal			
	BreadthFirst Search		DepthFirst Search		BreadthFirst Search		DepthFirst Search	
	# RLC	# TLC	# RLC	# TLC	# RLC	# TLC	# RLC	# TLC
Separable 2D Filter	22	35	17	35	22	35	17	35
sobel Filter	64	85	35	85	69	85	35	85

5) Tracking back:

In this step, the first map for the last simple mapped block will be chosen. The map you have chosen updates the limitations of current block mapping. At that point, if a mapping solution cannot be found for that base block due to the constraints, the builder will select the second map of the previous basis block to update the restriction and restart mapping of the current basis block. The method continues to correctly map the current basic block.

Annals of R.S.C.B., ISSN:1583-6258, Vol. 25, Issue 4, 2021, Pages. 4919 - 4942
Received 05 March 2021; Accepted 01 April 2021.

6) Update parameters:

A limit database is now developed and modified by the compiler. It is used to position data nodes and service nodes on a TLC and RLC basis in a placement algorithm. New variables cannot be applied to RLCs when mapping the current block, while TLCs are used to map symbolic variables. If in the current base block mapping database no symbolic variables remain, the variables are mapped so that the database can update until using the available resources the next basic block is mapped. The compiler produces a single-map assembly for the whole CDFG before all fundamental blocks are mapped.

Assembler

In the compilation of the PEA model and the actual hardware implementation, Assembler contains a key. It uses the ISA architecture and the ASCII text assembly for compiling and generates machine code which can serve as a hardware PE configuration. You can also adapt a PE. In addition to the PEA model used in the compiler, the ISA offers hardware expertise. For example, PEs uses a CRF file to save constants in the IPA. The CRF in the PEA model reduces the time of learning by saving instruction instantaneously in internal registers and offers a low power solution. This is how the assembler separates the model from the real compiler hardware implementation. The PEA model can be described and the architecture can be derived. Even for several PEA variants the compiler is suitable.

4. Results and Discussions

This section analyses how various signal processing kernels are efficient, field and power consumption. We conduct experiments to show that, compared to advanced prediction techniques; we are efficient in assigning registry to a wide range of managed kernels. An architectural exploration is also carried out in order to ensure optimal setup of load-storage units and TCDM banks for an IPA with 4X4 PE arrays. The performance and energy efficiency of the or1k-CPU is also compared.

4.1.Implementation

The results for IPA accelerators are discussed in this section and contrast to CSC1K. Both prototypes are compatibilized with the STMicroelectronics FD-SOI 28nm UTBB technology

Annals of R.S.C.B., ISSN:1583-6258, Vol. 25, Issue 4, 2021, Pages. 4919 - 4942
Received 05 March 2021; Accepted 01 April 2021.

library in the Synopsys Design Controller 2014.09-SP4. In standard production conditions for the 0.6V, 25C thermal delivery, Synopsys Prime Power 2013.12SP3 was used for timing and power analysis. Cycle data have been obtained in order to simulate RTL with Tutor Questa Sim-64 10.5c. A total of 4 list 16 PEs, all records as shown in the table 5, with 20 32-bit, 32 8-bit and 32 16-bit registrations. The CPU has a data memory of 32kB, 4kB instructions and a buffer of 1kB that is equal to IPA design parameters. Table 4 reveals all kernels for further studies in coding scale (instructions and constants).

The cost of the IRF is considered both in size and power. The IPA operates at a speed of 100 mhz, while the IPA operates at a speed of only 45 mhz at a single operating point on the target voltage of 0.6 V. The full memory array with a number of various TCDM banks, totaling 32 kB of memory, is shown in Figure 4. Compared with the entire device area with full PE arrays, the field results for the most severe scenario are insignificant (i.e. 16).

As shown in figure 4, IPA is the minimum configuration for four TCDM Banks with the array (60%) and local data (35%), while the remaining 5% are connected. The growing number of TCDM banks is putting a large overhead area on the interconnection scale. The TCDM region has also grown to cover 32 kB in several banks as a result of the wider area/bit of small SRAM cuts. Therefore, the number of LSUs and TCDM banks must be balanced against the application's bandwidth requirements.

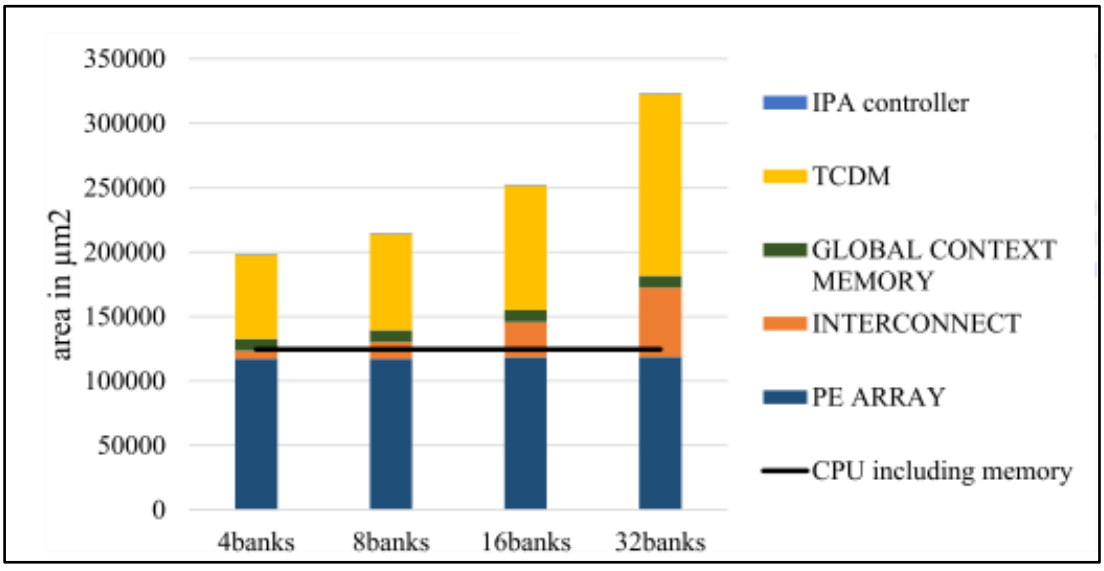

Figure 4: Area for various TCDM

Annals of R.S.C.B., ISSN:1583-6258, Vol. 25, Issue 4, 2021, Pages. 4919 - 4942
Received 05 March 2021; Accepted 01 April 2021.

Table 4: Code Size in IPA

Kernels	FIR	MatM	Conv	SepFilter	Non SepFilter	FFT	DCFilter	Cordic	Sobel	Gcd	Sad	Deblock	Manh-Dist
Code size (KB)	0.568	0.704	0.704	0.720	0.784	0.696	1.16	0.496	0.336	1.448	0.600	2.016	0.624
Max depth loop nests	2	3	3	3	4	2	2	1	1	1	2	3	2

Table 5: Memories used in IPA

Name	Type	Size
Global context memory	SRAM	8KB
TCDM	SRAM	32KB
Instruction Register File (IRF)	Registers	0.08KB
Regular register file (RRF)	Registers	0.032KB
Constant register fie(CRF)	Registers	0.128KB

Table 6: Performance Comparison

Kernels	# Loops	# Conditionals	Performance (cycles)					
			reg	SLS based	partial	full	CPU	C64
cordic	1	2	328	408	396	542	513	286
sobel	4	11	179 617	262 282	188 253	245 583	454 028	669 794
gcd	1	1	55 312	58 596	73 747	92 852	67 545	92 184
sad	2	1	15 962	16 824	16 573	28 776	62 932	252 193
deblocking	5	7	472 258	495 081	518 722	727 243	834 683	1 310 220
manh-dist	1	1	6 288	6 826	6 738	9 522	15 394	55 317
	max gain			1.46×	1.33×	1.8×	3.94×	15.8×

Annals of R.S.C.B., ISSN:1583-6258, Vol. 25, Issue 4, 2021, Pages. 4919 - 4942
Received 05 March 2021; Accepted 01 April 2021.

Kernels	Energy (µJ)					
	reg	SLS based	partial	full	CPU	C64
cordic	0.001	0.002	0.002	0.002	0.004	0.002
sobel	0.736	1.102	1	1.058	3.531	5.656
gcd	0.227	0.246	0.392	0.4	0.525	0.778
sad	0.065	0.071	0.088	0.124	0.489	2.13
deblocking	1.936	2.079	2.754	3.134	6.492	11.064
manh-dist	0.026	0.029	0.036	0.041	0.12	0.467
		2×	2×	2×	7.52×	32.77×

4.2. Comparison of Proposed Method

In order for the register assignment system to monitor the flow to determine the quality, we compare the output of six control kernels with the state of the art partial and full predictive methods. The results from Table 6 show that the record-based method has achieved a cumulative efficiency gains of 1,33x (minimum 1.04x and average 1.13x) and 1,8x (minimum 1,37x and average 1.59x) relative to partial forecasts and full forecasting techniques. The biggest benefit over existing procedures is the bold table. The average partial and full energy efficiency prediction is 1,54x (1.34x, max. 2x) and 1,71x with the smaller numbers of directions (1.44x, max. 1x). There is also a comparison between the TI or1k CPU and the C64 DSP processor in the table. For gross power gains of 3,94x, 15,8x, 7,52x, 32,77x and C64 processor in excess of or1k, the register assignment method shall be used. DSP is worse because of the proliferation of branches in the kernels. Finally, we compare the computer dependent approach to maps on the basis of simple load-stores (SLS). The average performance is 1.16x (maximum 1,46x, min. 1,05x) for registering with respect to the average SLS approach; the average energy efficiencies of 1.31x are 2x higher and a nominal improvement is 1.07x higher.

4.3. Architectural Experimentation

This section provides an overview of the CPU model machine and an IPA performance evaluation and adjusts the number of LSU and TCDM banks that are essential data-needing

Annals of R.S.C.B., ISSN:1583-6258, Vol. 25, Issue 4, 2021, Pages. 4919 - 4942
Received 05 March 2021; Accepted 01 April 2021.

acceleration parameters. To perform the exploration we chose 7 kernels that process signal intensives with a high bandwidth to TCDM.

4.3.1 Performance

In general, if the kernel can extract meaningful parallels, the IPA will work well, when array sizes are grown from 2x2 to 32x32 in matrix multiplication, compared IPA performance with the or1k processor performance. The increase in kernel size also enhances the medium usage of PEs, thus improving performance. It can also be found that the initial setup period prevailing over smaller kernels with larger kernels, which improves further performance, is well below anticipated. Fig. 5 defines the cumulative runtime of 7 computer-intensive kernels (clock cycles). The or1k processor runtime is standardized, where kernels have a -O3 optimization flag constructed. The IPA is up to 20.3 times higher with an average speed of 9.7x. A quantitative comparison of performance in the CPU is provided in Table 7. The table presents the setup and execution cycles for different IPA kernels. It also shows the average overall use of PEs as well as the total number of IPA instructions during the total period. The guide count provides instructions for keeping the PE synchronized with hops. All PEs are recurrent. It also involves NOPs when the PEs has been stuck due to manipulation of index variables. However, PEs do not consume dynamic power when executing NOPs and are clock resistant. The IPA achieves an energy gain of 18 times and 9.23 times over the CPU. Within the PE range we differ in 4 to 16 LSUs from 4 to 32 TCDM banks, which evaluate the output and energy efficiency impact of the memory bandwidth. The LSU count determines the amount of bandwidth that TCDM will collect, while the increased number of TCDM banks decreases the possibility of bank disputes and increases efficiency. Inside the kernel's innermost loops a maximum of 16 load storage operations are carried out in one cycle without distinguishing the settings (as the highest number of LSUs considered is 16, in the exploration). In figure 5 each set is represented as a two-dimensional number, with the first as an LSU and the second as a TCDM.

Results indicate, in comparison with closely connected processor clusters which demand a banking factor of two, that IPA results are almost indifferent to a bank of TCDM and a bank factor of 0.5 to reduce the effects of conflict on the common memory banks for most applications (i.e. the number of TCDM banks twice the cores). If the variables above the register file size require several load/storage operations while standard processor executions require the direct

Annals of R.S.C.B., ISSN:1583-6258, Vol. 25, Issue 4, 2021, Pages. 4919 - 4942
Received 05 March 2021; Accepted 01 April 2021.

CDFG mapping to IPA does not add more storage activities other than the primary inputs and outputs because all of the time variables are stored on the PE register. Furthermore, the multi-faceted link in the array enables the efficient exchange of data between PEs and reduces the burden of TCDM further.

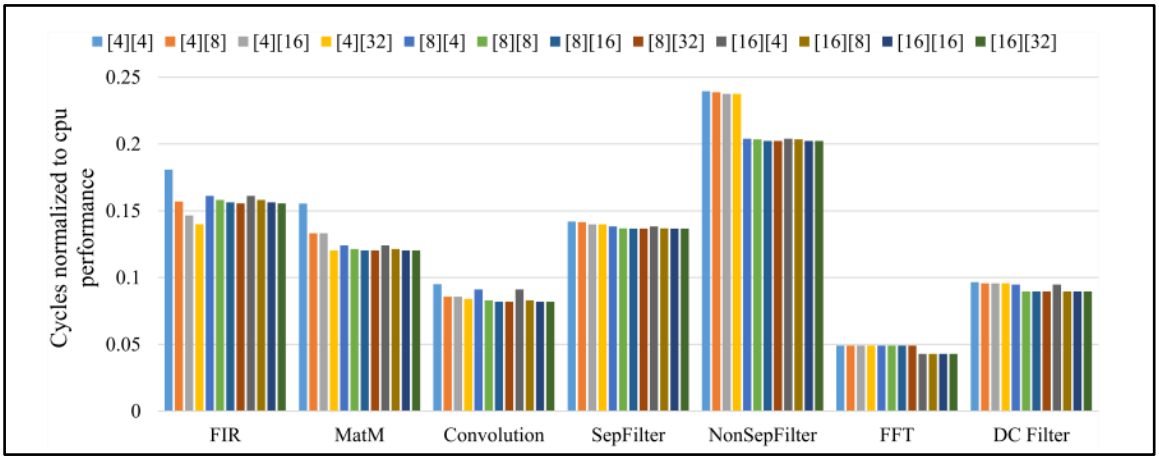

Figure 5: Performance comparison

Table 7: Energy consumption IPA vs CPU

Kernels		FIR	MatM (16×16)	Convolution	SepFilter	NonSepFilter	FFT	DC Filter
IPA	Configuration cycles	71	88	88	90	98	87	145
	Execution cycles	6071	11940	56241	827685	1852382	8076	4748
	Total number of instructions executed	44294	110946	531815	7349843	17486486	76310	28868
	Active PEs/cycle (%)	46.1	58.5	59.2	55.5	59	59.7	39.5

Annals of R.S.C.B., ISSN:1583-6258, Vol. 25, Issue 4, 2021, Pages. 4919 - 4942
Received 05 March 2021; Accepted 01 April 2021.

	Energy (µJ)	0.022	0.043	0.202	2.98	6.669	0.032	0.017
	Energy (µJ) in non-clock-gated IPA	0.047	0.077	0.479	7.152	11.704	0.063	0.045
CPU	Execution cycles	37677	96256	616805	598230	9084101	164480	50085
	Energy (µJ)	0.132	0.337	2.159	20.94	31.794	0.576	0.175
	Speed-up	6.21x	8.06x	10.97x	7.23x	4.9x	20.3x	10.55x
	Energy-gain	6x	7.84x	10.69x	7.03x	4.77x	18x	10.29x

4.3.2Energy efficiency

The average power consumption decay for different IPA settings is shown in Figure 6. For all setups, PE is the dominant power consumer. The four TCDM banks offer each group the best energy benefits as the increased complexity of the interconnection increases the number of banks, thus generating chronological strain on the cell size range that increases the consumption of electricity. Figure 7 screens for various average configurations of energy efficiency. MOPS cannot take into account TCDM banking access, active NOPs or unmapped access unless PE is successful (not used in the application execution). MOPS substantially increase high-quota PE/cycle outputs. The four TCDM bank configurations represents the best energy efficiency for different LSU numbers in the PE series, since the smallest number of banks in each configuration decreases the energy consumption. At the same time, because of a lower memory access strategy, the active number of PEs/cycles has no noticeable effect. It means that the best possible efficiency in a configuration with 8 LSU and 4 TCDM banks can be achieved for matrix

Annals of R.S.C.B., ISSN:1583-6258, Vol. 25, Issue 4, 2021, Pages. 4919 - 4942
Received 05 March 2021; Accepted 01 April 2021.

multiplication at 2306 MOPS/mW. For separate filters of 4 LSU configuration and 16 TCDM banks, minimum energy efficiency is achieved at 1112 MOPS/mW.

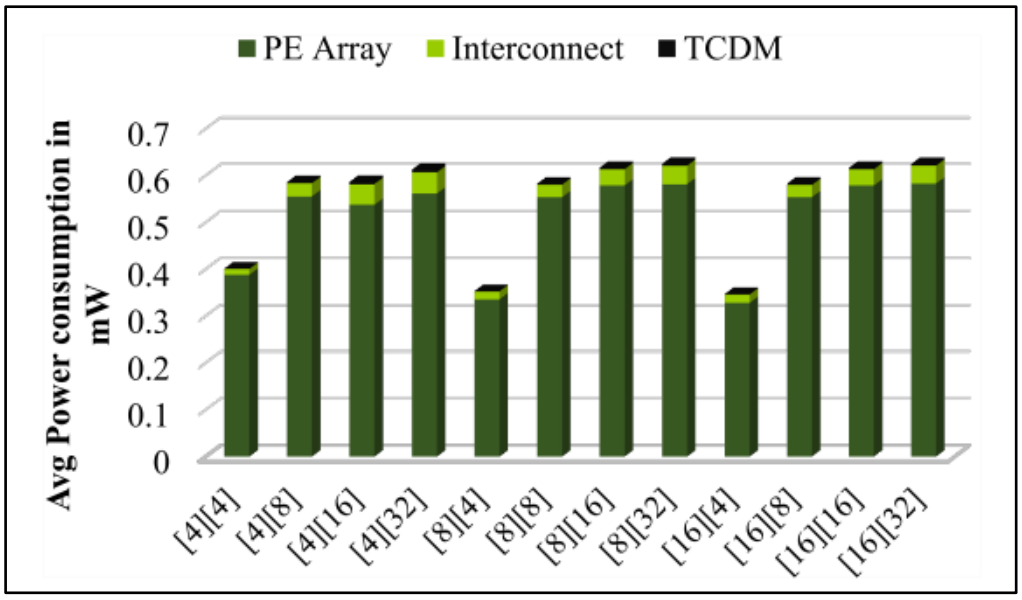

Figure 6: Average Power Breakdown

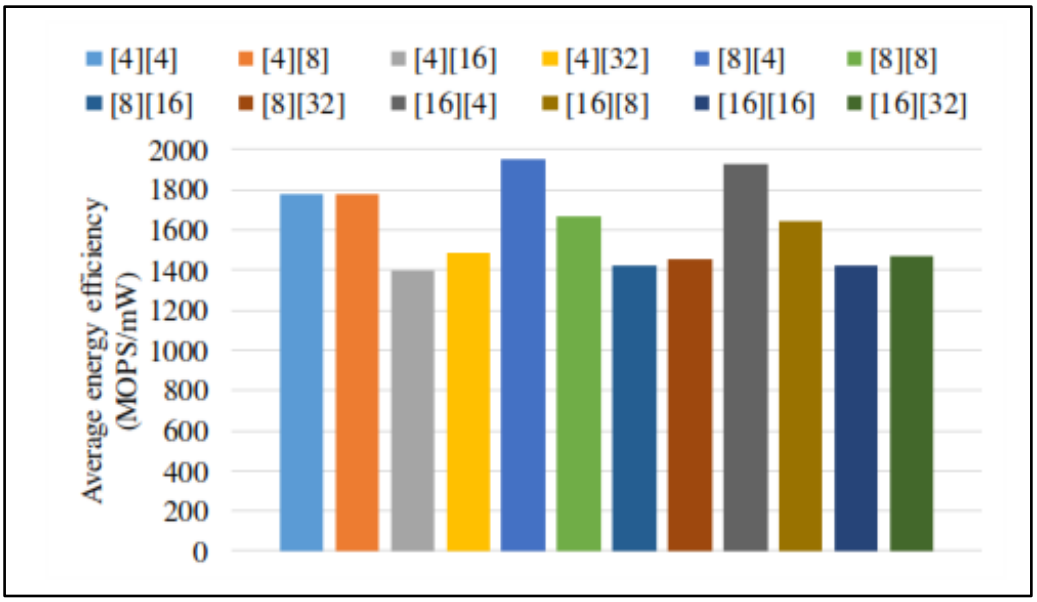

Figure 7: Average energy efficiency

Table 7 displays the energy usage for a clock-gated IPA and non-clock-gated IP A for the study of fine grain clock-ratio energy savings. The clock-door system uses on average 2 times less power than the non-clock-gated-door design. Thanks to the standard PE architecture, the fine seed power control is much simpler than a processor. In addition, the IPA's energy efficiency is

Annals of R.S.C.B., ISSN:1583-6258, Vol. 25, Issue 4, 2021, Pages. 4919 - 4942
Received 05 March 2021; Accepted 01 April 2021.

up to 18x at or above the 1K processor at CDFG efficiency range and fine-grained energy management reliability with lower energy requirements (5.6E-08 J vs. 3.49E-06 J) at IPA instructions for CPUs. Thanks to its simple instructional set architecture, the IPA energy per instruction is significantly less than the CPU. Moreover, the lower IPA memory number decreases the total usage of resources.

5. Conclusion

This task includes a highly configurable, extremely low power accelerator near-sensor. The proposed Integrated Programming Array (IPA) is a 2D array of NxN Processing Components that makes it easier to implement data storage with multitasking and tightly linked data storage in clustered multi-core architectures. We add a compiled flow to the mapping part of the control and data flow in order to reduce the burden on the common data memory and architecturally calculate the memory architecture parameters. The research showed that the optimum energy/performance balance was 9,7x (max 20,3x, min 4,9x) in a mean speed relative to the overall IPA set-up, with 8 load storage units and four TCDM benches. The proposed compilation flow has increased the average power output by 1.54 time (1.35, max 2x) and the average power output by 1.71x in new, partial and full prediction techniques (min 1.44x, max 2x). With a wider range of signal handling sensor nodes with an optimised design and mapping flow exceeding one order in other CGR A architectures with a C mapping flow, the accelerator proposed achieved an average energy efficiency of 1617 MOPS/mW.

References

[1] F. Glaser, G. Tagliavini, D. Rossi, G. Haugou, Q. Huang and L. Benini, "Energy-Efficient Hardware-Accelerated Synchronization for Shared-L1-Memory Multiprocessor Clusters," in IEEE Transactions on Parallel and Distributed Systems, vol. 32, no. 3, pp. 633-648, 2021.

[2] A. Lamzed-Short, T. R. Law, A. Mallinson, G. R. Mudalige and S. A. Jarvis, "Towards Automated Kernel Fusion for the Optimisation of Scientific Applications," 2020 IEEE/ACM 6th Workshop on the LLVM Compiler Infrastructure in HPC (LLVM-HPC) and Workshop on Hierarchical Parallelism for Exascale Computing (HiPar), GA, USA, 2020.

Annals of R.S.C.B., ISSN:1583-6258, Vol. 25, Issue 4, 2021, Pages. 4919 - 4942
Received 05 March 2021; Accepted 01 April 2021.

[3] B. Wang, M. Karunarathne, A. Kulkarni, T. Mitra and L. Peh, "HyCUBE: A 0.9V 26.4 MOPS/mW, 290 pJ/op, Power Efficient Accelerator for IoT Applications," 2019 IEEE Asian Solid-State Circuits Conference (A-SSCC), Macau, Macao, 2019.

[4] D. Rossi, A. Pullini, I. Loi, M. Gautschi, F. K. G urkaynak, A. Bartolini, P. Flatresse, and L. Benini. A 60 GOPS/W, -1.8 V to 0.9 V body bias ULP cluster in 28 nm UTBB fd-soi technology.Solid-State Electronics, 117:170 – 184, 2016.

[5] S. Das, D. Rossi, K. Martin, P. Coussy, and L. Benini. A 142 mops/mw integrated programmable array accelerator for smart visual processing. In 2017 IEEE International Symposium of Circuits and Systems (ISCAS), page Accepted, 2017.

[6] Z. E. Rakossy, A. Acosta-Aponte, T. G. Noll, G. Ascheid, R. Leupers, and A. Chattopadhyay. Design and synthesis of reconfigurable controlflow structures for cgra. In 2015 International Conference on ReConFigurable Computing and FPGAs (ReConFig), p.1–8, 2015.

[7] S. Yin, P. Zhou, L. Liu, and S. Wei.Acceleration of nested conditionals on cgras via trigger scheme. In Proceedings of the IEEE/ACM International Conference on Computer-Aided Design. IEEE Press, 2015.

[8] B. De Sutter, P. Raghavan, and A. Lambrechts.Coarse-grained reconfigurable array architectures. In S. S. Bhattacharyya, E. F. Deprettere, R. Leupers, and J. Takala, editors, Handbook of Signal Processing Systems, pages 449–484. Springer US, 2010.

[9] F. Bouwens, M. Berekovic, A. Kanstein, and G. Gaydadjiev.Architectural exploration of the adres coarse-grained reconfigurable array. In Proceedings of the 3rd International Conference on Reconfigurable Computing: Architectures, Tools and Applications, ARC'07, 2007.

[10] M. Hamzeh, A. Shrivastava, and S. Vrudhula.Regimap: register-aware application mapping on coarse-grained reconfigurable architectures (cgras). In Proceedings of the 50th Annual Design Automation Conference, page 18. ACM, 2013.

[11] D. Liu, S. Yin, L. Liu, and S. Wei. Polyhedral model based mapping optimization of loop nests for cgras. In Design Automation Conference (DAC), 2013 50th ACM/EDAC/IEEE, pages 1–8. IEEE, 2013.

Annals of R.S.C.B., ISSN:1583-6258, Vol. 25, Issue 4, 2021, Pages. 4919 - 4942
Received 05 March 2021; Accepted 01 April 2021.

[12] C. Liu, H. Ng, and H. K. So. Automatic nested loop acceleration on fpgas using soft CGRA overlay. CoRR, abs/1509.00042, 2015.

[13] K. Han, S. Park, and K. Choi.State-based full predication for low power coarse-grained reconfigurable architecture. In 2012 Design, Automation Test in Europe Conference Exhibition (DATE), March 2012.

[14] M. Balasubramanian and A. Shrivastava, "CRIMSON: Compute-Intensive Loop Acceleration by Randomized Iterative Modulo Scheduling and Optimized Mapping on CGRAs," in IEEE Transactions on Computer-Aided Design of Integrated Circuits and Systems, vol. 39, no. 11, pp. 3300-3310, Nov. 2020.

[15] L. Liu, J. Wang, J. Zhu, C. Deng, S. Yin, and S. Wei.Tlia: Efficient reconfigurable architecture for control-intensive kernels with triggered long-instructions. IEEE Transactions on Parallel and Distributed Systems,27(7):2143–2154, July 2016.

[16] S. Das, K. J. M. Martin, P. Coussy, D. Rossi, and L. Benini.Efficient mapping of CDFG onto coarse-grained reconfigurable array architectures. In 2017 22nd Asia and South Pacific Design Automation Conference (ASP-DAC), pages 127–132, Jan 2017.

[17] H. K. Nguyen and M. T. Phan, "RTL design of a dynamically reconfigurable cell array for multimedia processing," 2017 4th NAFOSTED Conference on Information and Computer Science, Hanoi, 2017, pp. 189-194.

[18] S. Das, T. Peyret, K. Martin, G. Corre, M. Thevenin, and P. Coussy. A scalable design approach to efficiently map applications on CGRAs. In 2016 IEEE Computer Society Annual Symposium on VLSI (ISVLSI), pages 655–660, July 2016.

[19] T. Peyret, G. Corre, M. Thevenin, K. Martin, and P. Coussy. Efficient application mapping on cgras based on backward simultaneous scheduling/binding and dynamic graph transformations. In 2014 IEEE 25th International Conference on Application-Specific Systems, Architectures and Processors, pages 169–172.IEEE, 2014.

[20] Awchat, G. D., and Yamini N. Deshmukh. "Seismic Response of Tall Building with Underground Storey Using Dampers." International Journal of Civil Engineering (IJCE) 6.4 (2017): 57 66.

[21] Kulkarni, Mr Prashant Kadi1 Mr Shrirang, and Prashant Kadi. "Hybrid Powered Electric Bicycle." 2016 International Journal for Scientific Research and Development Vol 4.

[22] Yadav, Vivek Kumar, and Navjot Bhardwaj. "Regenerative braking for an electric vehicle using hybrid energy storage system." International Journal of Electrical and Electronics Engineering Research (IJEEER) 3.4 (2013): 35-42.

[23] Xydou, A., et al. "Production of CLIC accelerating structures using diffusion bonding at very high temperature." Int. Journal of Mettalurgical and Materials Science and Engineering (IJMMSE) 6.2 (2016).

[24] Gopalakrishna, H. D., et al. "Crashworthiness of Automobile in a Vehicle-to-Pole Crash Simulation." International journal of automobile engineering research & development, ISSN (E) (2014): 2278-9413.

[25] PREMKUMAR, M., et al. "Design, analysis and fabrication of solar pv powered bldc hub motor driven electric car." Inter. J. Mecha. Produc. Engi. Res. Develop 8.1 (2018): 1255-1270.